

# Extended reionization in models beyond $\Lambda$ CDM with Planck 2018 data

Daniela Paoletti,<sup>1,2</sup> Dhiraj Kumar Hazra,<sup>3,1,2</sup> Fabio Finelli,<sup>1,2</sup>  
George F. Smoot<sup>4,5,6,7</sup>

<sup>1</sup>Osservatorio di Astrofisica e Scienza dello Spazio di Bologna/Istituto Nazionale di Astrofisica, via Gobetti 101, I-40129 Bologna, Italy

<sup>2</sup>Istituto Nazionale Di Fisica Nucleare, Sezione di Bologna, Viale Berti Pichat, 6/2, I-40127 Bologna, Italy

<sup>3</sup>The Institute of Mathematical Sciences, HBNI, CIT Campus, Chennai 600113, India

<sup>4</sup>Paris Centre for Cosmological Physics, Université de Paris, CNRS, Astroparticule et Cosmologie, F-75013 Paris, France

<sup>5</sup>Institute for Advanced Study & Physics Department, Hong Kong University of Science and Technology, Clear Water Bay, Kowloon, Hong Kong

<sup>6</sup>Physics Department and Lawrence Berkeley National Laboratory, University of California, Berkeley, CA 94720, USA

<sup>7</sup>Energetic Cosmos Laboratory, Nazarbayev University, Astana, Kazakhstan

E-mail: [daniela.paoletti@inaf.it](mailto:daniela.paoletti@inaf.it), [dhiraj@imsc.res.in](mailto:dhiraj@imsc.res.in), [fabio.finelli@inaf.it](mailto:fabio.finelli@inaf.it), [gfsmoot@lbl.gov](mailto:gfsmoot@lbl.gov)

**Abstract.** We provide an update on the constraints on extended reionization histories with the Planck 2018 cosmic microwave background anisotropy data. The Planck 2018 data on large angular scales improve the measurement of the  $E$ -mode polarization reionization bump at low multipoles providing the possibility to improve our previous results [1]. Using a minor modification to the original Poly-reion model [2] for the reionization history, we find that the Planck 2018 data significantly improve all our previous results: we find an optical depth of  $\tau = 0.0572^{+0.0064}_{-0.0075}$  at 68% CL, that early onsets of reionization are strongly disfavoured, i.e. redshift when the reionization begins,  $z_{xe=0} = 18.18^{+1.61}_{-10.89}$  at 68% CL, and that reionization duration (defined between 10% and 99% reionization) is significantly reduced, i.e.  $\Delta_z^{Reion} = 4.59^{+1.67}_{-2.45}$  at 68% CL. We explore possible correlations between reionization histories and cosmological parameters, including important extensions beyond  $\Lambda$ CDM. We find that the degeneracy between reionization and scalar spectral index, neutrino mass sum, spatial curvature, dark matter annihilation and other non-standard models are significantly reduced. The reduction of the error bars and the degeneracies, together with the shift towards lower values of the optical depth that we observe in the Poly-reion model are mainly driven by the new low- $\ell$  polarization likelihood of Planck 2018 baseline based on the HFI data. This is confirmed also by the results derived without this likelihood and the ones with different alternatives to the baseline that are presented for a subset of models.

---

## Contents

<b>1</b>	<b>Introduction</b>	<b>1</b>
<b>2</b>	<b>Poly-reion model for the history of reionization</b>	<b>2</b>
<b>3</b>	<b>Constraints on the history of reionization with Planck 2018</b>	<b>3</b>
3.1	Planck 2018 baseline	3
3.2	Alternatives to Planck 2018 baseline	5
<b>4</b>	<b>Extensions to the <math>\Lambda</math>CDM</b>	<b>9</b>
4.1	$\Lambda$ CDM+tensor	9
4.2	Neutrino Physics	10
4.2.1	$\Lambda$ CDM+Mnu	10
4.2.2	$\Lambda$ CDM+ $N_{eff}$	11
4.2.3	$\Lambda$ CDM+Neff+Mnu	12
4.3	$\Lambda$ CDM+ $A_L$	12
4.4	$\Lambda$ CDM+curvature	13
4.5	Large scale power suppression	14
4.6	$\Lambda$ CDM+DM annihilation	15
<b>5</b>	<b>Conclusions</b>	<b>16</b>

---

## 1 Introduction

Reionization marks the end of the dark ages, with the first sources of ionizing photons lighting up. The CMB anisotropy pattern is a main source of information on the reionization process. Its sensitivity to the details of reionization originates from two different effects: 1) the opacity generated by reionization suppresses the power of CMB anisotropies because of the rescattering of photons (this effect is at the basis of the degeneracy between the amplitude of primordial fluctuations and the optical depth); 2) the rescattering of the photon quadrupole generates a bump at the multipoles below ten in the CMB polarization anisotropies. The reionization bump in the E-mode polarization provides information on both the value of the (average) optical depth, that is related to its amplitude, and to a lesser extent on the duration of reionization, that is instead related to the shape of the bump.

The latest results in CMB polarization anisotropy measurements by Planck [3–5] have shed light on the reionization process. The Planck 2018 determination of the (average) optical depth is [5]  $\tau = 0.054 \pm 0.007$  (TTTEEE+lowE+lensing) at 68 % CL. Being the average optical depth the one of the six cosmological parameter of the  $\Lambda$ CDM cosmology with the largest uncertainty, it is a standard approximation to compress the CMB information on reionization in the (effective) redshift at which it occurred by adopting an hyperbolic tangent variation in the ionization fraction, which is therefore determined as  $z_{re}$  at 68 %CL.

With these recent CMB polarization measurements the constraints on reionization beyond the simple hyperbolic tangent model used as baseline in cosmology have also significantly improved. These investigations include physical models for the reionization history [4] or a pure free form data fitting with principal component analysis [6, 7], to hybrid parametric fitting models [2, 5, 8] and astrophysical data driven reconstructions [9–11].

The analysis of CMB anisotropy data beyond the optical depth are not relevant only for the understanding of the physics of reionization, because of its known and possible degeneracy with other cosmological parameters [12, 13], as for instance with the amplitude of the power spectrum of primordial perturbations. The situation gets more complex when we open up to extensions of the standard cosmological model as in [1], where the degeneracy with neutrino sector and DM annihilation are studied. The same situation arises also for the study of alternative choices of the primordial power spectrum as in the search for primordial features, where as shown in [14, 15] the uncertainty on the reionization process diminishes the significance of possible detections.

In this work we update with Planck 2018 data our previous constraints on the parametric model of reionization *termed* Poly-reion [1] not only within  $\Lambda$ CDM, but also within several extended cosmological models to search for potential degeneracies of the physics of reionization with extra cosmological parameters beyond  $\Lambda$ CDM. In addition to Planck 2018 data, we also use the reprocessing of large scale Planck HFI polarization data from [16].

The article is organized as follows. In section 2 we describe the Poly-reion model in the form used in this work. In section 3 we present the results for the standard cosmological model with different combination of Planck 2018 likelihoods and the more recent reprocessing of Planck HFI large scale polarization data from Planck [16]. In section 4 we present the results of the Planck 2018 baseline for the main extensions to the standard cosmological model. We conclude in Section 5.

## 2 Poly-reion model for the history of reionization

In order to go beyond the standard hyperbolic tangent model for  $x_e$ , we use the Poly-reion model of reionization. Poly-reion was originally introduced in [2], it interpolates the ionization fraction between different nodes; in its original version it assumed fixed nodes at different redshifts, thereafter instead it used flexible nodes as in [1, 14]. Poly-reion uses Piecewise Cubic Hermite Interpolating Polynomial (PCHIP) [17] to interpolate the free electron fractions ( $x_e(z)$ ) between different nodes in the redshift space. We use four nodes, the first two are fixed by assuming that the reionization is completed by redshift ( $z$ ) 5.5<sup>1</sup> and the Universe remained completely ionized till date [19], namely we fix the  $z = 0$  and  $z = 5.5$  nodes. The other two nodes consider a flexible intermediate node called  $z_{int}$  and  $z_{x_e=0}$  which denotes the redshift where the reionization begins and  $x_e = 0$ . In the intermediate node we vary both the position in redshift and the amplitude of the ionization fraction:  $z_{int}$  is allowed to vary between 5.5 and 30 and  $x_e(z)$  takes the values between 0 and 1. Given  $z_{int}$  and  $x_e(z_{int})$ , we solve for  $z_{x_e=0}$  for a value of optical depth  $\tau$  between  $z_{int}$  and a very high redshift ( $z = 70$  in our case). Together with the position and amplitude of the intermediate node  $z_{int}$  and  $x_e(z_{int})$ , the optical depth represents the third parameter describing the reionization in our model and we vary it with a uniform prior.

By construction this model of Poly-reion allows only monotonic reionization, in fact, the use of PCHIP in the interpolation guarantees the consistency of the electron fraction which can vary only between the physical values 0 and 1 as this Polynomial preserves the form. We note anyway that monotonic histories have been shown to be the most favoured by CMB and astrophysical data [10]. The reionization history constructed with Poly-reion is used only for hydrogen reionization in our work. We assume that Hydrogen reionization is completed by  $z = 5.5$  concerning the other two steps of reionization regarding Helium I and Helium II, we assume the standard hyperbolic tangent form with the first helium reionization at the same time as the hydrogen and the second at redshift of 3.5

---

<sup>1</sup>While in most cases  $z = 6$  is considered to be the completion of reionization, we use 5.5 to be conservative following analyses that suggest the possible presence of reionization at  $z < 6$  [18]

as in Planck baseline. The standard model assumed for reionization is the hyperbolic tangent whose standard form assumes:

$$x_e(z) = \frac{1 + F_{\text{He}}}{2} \left[ 1 + \tanh \left( \frac{y(z_{\text{re}}) - y(z)}{\delta_{\text{reion}}} \right) \right], \quad (2.1)$$

where  $y(z) = (1+z)^{3/2}$ ,  $\delta_{\text{reion}} = 1.5 \sqrt{1+z_{\text{re}}} dz$ .  $z_{\text{re}}$  denotes the redshift at which this symmetric model of reionization is halfway complete.  $F_{\text{He}}$  is calculated from mass fraction of helium consistent with Big Bang Nucleosynthesis. Standard analysis assumes  $dz = 0.5$  which is also used in the *Planck* grid results.<sup>2</sup>

Poly-reion with respect to the hyperbolic tangent allows for a much greater freedom and encompasses from near-instantaneous to very extended reionization histories, where we define the duration of reionization as the difference between the redshifts where reionization was 10% and 99% done. This freedom translates in a general preference for higher optical depths with respect to the hyperbolic tangent case, although always in agreement inside the error bars, due to the non-instantaneous duration of reionization allowed by the model.

### 3 Constraints on the history of reionization with Planck 2018

The section is dedicated to the constraints on the Poly-reion model for reionization with Planck 2018 data in the context of the  $\Lambda$ CDM model.

#### 3.1 Planck 2018 baseline

We start by considering the different combinations of the Planck 2018 baseline likelihood [20]. This choice of likelihoods contains a part at low- $\ell$ , i.e.  $2 \leq \ell \leq 29$ , whose temperature part uses a Gibbs sampler on a foreground cleaned combination of 30–353 GHz channels obtained by the `commander` algorithm and whose  $E$ -mode polarization is based on the 100x143 GHz cross angular power spectra. At high multipoles, the Plik TTTEEE includes auto and cross-spectra in temperature and polarization of 100, 143 and 217 GHz channels. The Planck 2018 baseline likelihood contains also the CMB lensing likelihood [21], in the conservative range  $8 \leq \ell \leq 400$ . For more details on these likelihoods see [20, 21].

We briefly summarize the improvements of the Planck 2018 data with respect to the 2015 release. The one that mostly affects the reionization history constraints is the change in the large angular scale polarization [20]. In Planck 2015 the baseline choice was provided by a pixel based TQU likelihood, whose polarization part was provided the Low Frequency Instrument (LFI) 70GHz channel cleaned by synchrotron and dust contamination with 30 GHz and 353 GHz, respectively. In 2018 the lowE likelihood is provided by a simulation based likelihood that uses the High Frequency Instrument (HFI) 100x143 GHz cross-spectra, significantly reducing the error bars and updating the 2016 first results [3]. Other important differences are the use of only *Planck* data in the Commander map for the 2018 Gibbs low- $\ell$  likelihood and at high multipoles temperature to polarization leakage corrections, that has validated the use of high- $\ell$  polarization and temperature-polarization cross-correlation for cosmological results.

The results from the Planck TTTEEE+lowE+lensing are shown in red in Fig. 1 and presented in the first column of Table 1. The results are consistent with the overall trend shown also by other extended models of reionization: with HFI low- $\ell$  polarization the duration of reionization allowed by Planck 2015 is strongly reduced [4, 5, 8, 10]. With current data the Poly-reion model is consistent with a shorter duration of reionization given by  $\Delta_z^{\text{Reion}} = 4.6_{-2.5}^{+1.7}$  at 68% CL and excludes very early

<sup>2</sup><http://www.cosmos.esa.int/web/planck/pla>

onsets  $z_{xe=0} = 18.2^{+1.7}_{-10.9}$  at 68% CL. The optical depth is in agreement with the hyperbolic tangent results with the tendency already shown in [1] for preferring higher central values  $\tau = 0.0572^{+0.0064}_{-0.0075}$  at 68% CL, compared to the Planck result  $\tau = 0.0544 \pm 0.0073$  [5]. Overall we note the significant improvements on the constraints on Poly-reion with respect to 2015 data [1] and the excellent consistency of the estimate of the remaining cosmological parameters with the standard use of the hyperbolic tangent case.

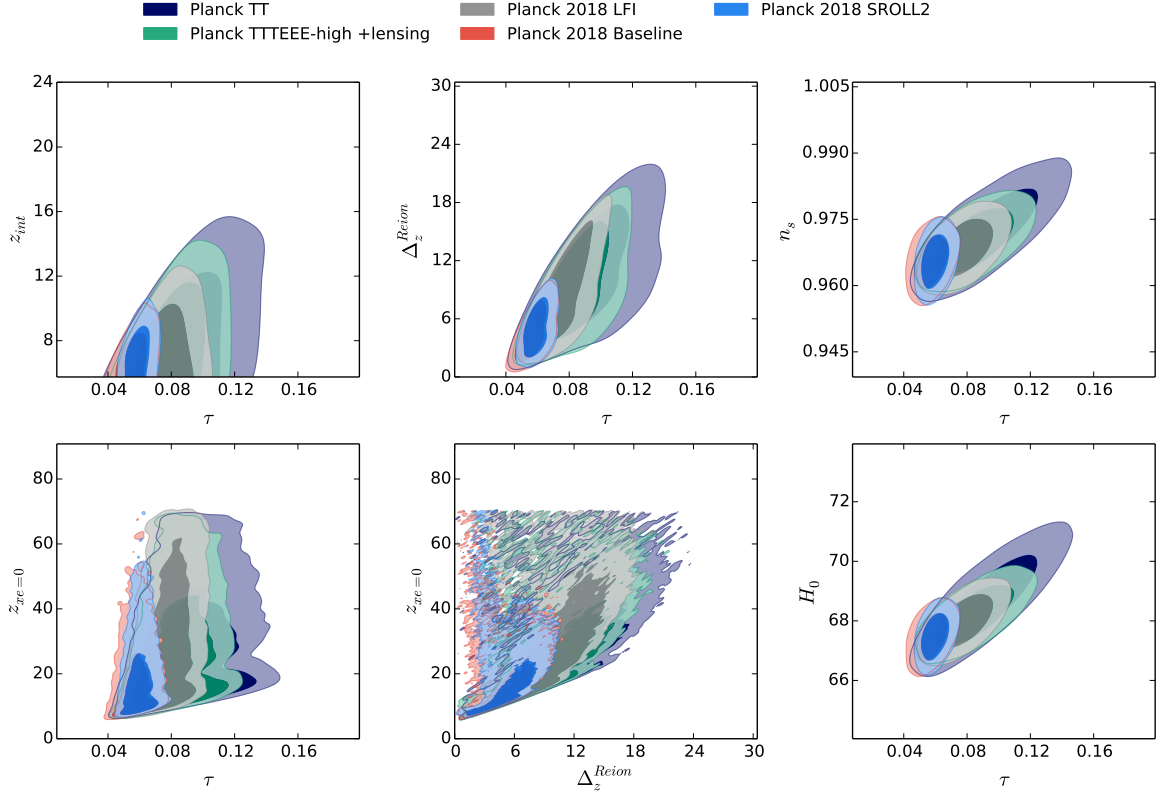


**Figure 1:** Marginalized joint 68% and 95% CL regions for cosmological and reionization parameters for different *Planck* 2018 likelihoods.

Parameter/Data	Planck TTTEEE + lowE+ lensing	Planck TT+lensing	Planck TTTEEE +lensing
$\Omega_b$	$0.0224 \pm 0.0001$	$0.0224 \pm 0.0002$	$0.0225 \pm 0.0002$
$\Omega_c$	$0.120 \pm 0.001$	$0.117 \pm 0.002$	$0.118 \pm 0.001$
$100\theta_{MC}$	$1.0409 \pm 0.0003$	$1.0412 \pm 0.0005$	$1.0411 \pm 0.0003$
$\tau$	$0.0572^{+0.0064}_{-0.0075}$	$0.0926^{+0.0196}_{-0.0232}$	$0.0851^{+0.0158}_{-0.0157}$
$\ln(10^{10}A_s)$	$3.05 \pm 0.01$	$3.11 \pm 0.04$	$3.10 \pm 0.03$
$n_s$	$0.9656 \pm 0.0041$	$0.9723 \pm 0.0065$	$0.9702 \pm 0.0048$
$H_0$	$67.46 \pm 0.54$	$68.67^{+0.99}_{-1.12}$	$68.21 \pm 0.66$
$z_{re}$	$7.24^{+0.74}_{-1.11}$	$9.40^{+1.69}_{-2.81}$	$8.90^{+1.55}_{-2.28}$
$z_{xe=0}$	$18.18^{+1.61}_{-10.89}$	$28.24^{+6.14}_{-18.28}$	$26.97^{+5.65}_{-17.62}$
$\Delta_z^{Reion}$	$4.59^{+1.67}_{-2.45}$	$10.47^{+3.92}_{-5.13}$	$9.43^{+3.57}_{-4.44}$

**Table 1:** Confidence limits (68 %) for cosmological parameters with different *Planck* 2018 likelihood combinations.

In order to fully understand our results, we investigate the variation of the angular power spectra in polarization and TE cross correlation with the Poly-reion parameters. In particular we study the variation with respect to the best fit of our results varying the three main parameters within 1 sigma of the data constraints: the position of the intermediate point  $z_{int}$  between [5.75,7.60], the amplitude of the ionization fraction in the the point  $x_{e=z_{int}}$  between [0.0665,0.674], the optical depth  $\tau$  between [0.0497,0.0632]. In Fig 2 we show the variation compared with the cosmic variance for a Planck-like experiment (70% of the sky coverage). The varied parameter is shown in the colormap, all the other parameters are fixed to their best fit value.

In order to test the different pulls data have on the Poly-reion model and the robustness of the results, we have considered different combinations of Planck baseline data subsets. We start by excising the large angular scale polarization from the likelihood combination. We consider only temperature data and use the leverage of the lensing to constrain the optical depth without imposing a Gaussian prior. The results are shown in purple contours in Fig. 1 and presented in the second column of Table 1. We first note the good agreement of the temperature plus lensing results with the baseline, though with an higher central value the optical depth is in agreement within 2 sigma. The addition of high-ell polarization tightens the error bars and pushes the optical depth towards lower values as shown by the green contours in Fig. 5 and the third column of Table 1.

### 3.2 Alternatives to Planck 2018 baseline

We test now the two available alternative likelihoods to the Planck 2018 baseline for large scale polarization. In the 2018 release together with the LowE likelihood it has been released a full TQU pixel based likelihood from the LFI data at 70 GHz (plus the same temperature map as lowI), lowTEB (note that a joint likelihood LFI-WMAP has been recently developed in [22]). This alternative likelihood is relevant, although it produces larger error bars, because it considers all the channels, TT, EE, BB and also TE, where the latter is not present in the baseline lowE, and it represents both a change in the data and a change in the likelihood algorithm, providing therefore an optimal robustness test. The results of this alternative likelihood are represented by the grey contours in Fig. 1. Considering the larger error bars the optical depth  $\tau = 0.078 \pm 0.012$  at 68% CL shows a very good agreement with the HFI based baseline, although with a slightly larger central value, a tendency shown also by the hyperbolic tangent.

We also test the alternative re-processing of Planck HFI data based on the SROLL2 map making algorithm [16] which reports an improvement in the removal of systematics with respect to the baseline Planck 2018 data analysis. The  $\Lambda$ CDM+ Tanh optical depth given by this likelihood, without the lensing addition, is  $\tau = 0.0590^{+0.0058}_{-0.0068}$  at 68% CL [23] with a slightly larger central value with respect to the Planck 2018 baseline result. We confirm this tendency towards higher values also with the Poly-reion model where we obtain  $\tau = 0.0600^{+0.0052}_{-0.0064}$ . The result is shown in blue in Fig. 1 and is in good agreement with the hyperbolic tangent case though with a slightly improved error bars given by the addition of the lensing likelihood which is not present in the hyperbolic tangent result.

In summary, the Planck 2018 data show a large improvement in the constraints to the Poly-reion model thanks mainly to the improved polarization on large angular scales. Long duration of reionization and early onsets, hinted by Planck 2015 data, are now strongly disfavoured with  $\Delta_z^{Reion} = 4.6^{+1.7}_{-2.5}$  at 68% CL and  $z_{x_{e=0}} = 18.2^{+1.7}_{-10.9}$  at 68% CL. The optical depth is in agreement with the hyperbolic tangent case with a slightly higher value  $\tau = 0.0572^{+0.0064}_{-0.0075}$  at 68% CL. The results are consistent against subsets of Planck data and alternatives to the baseline demonstrating the robustness

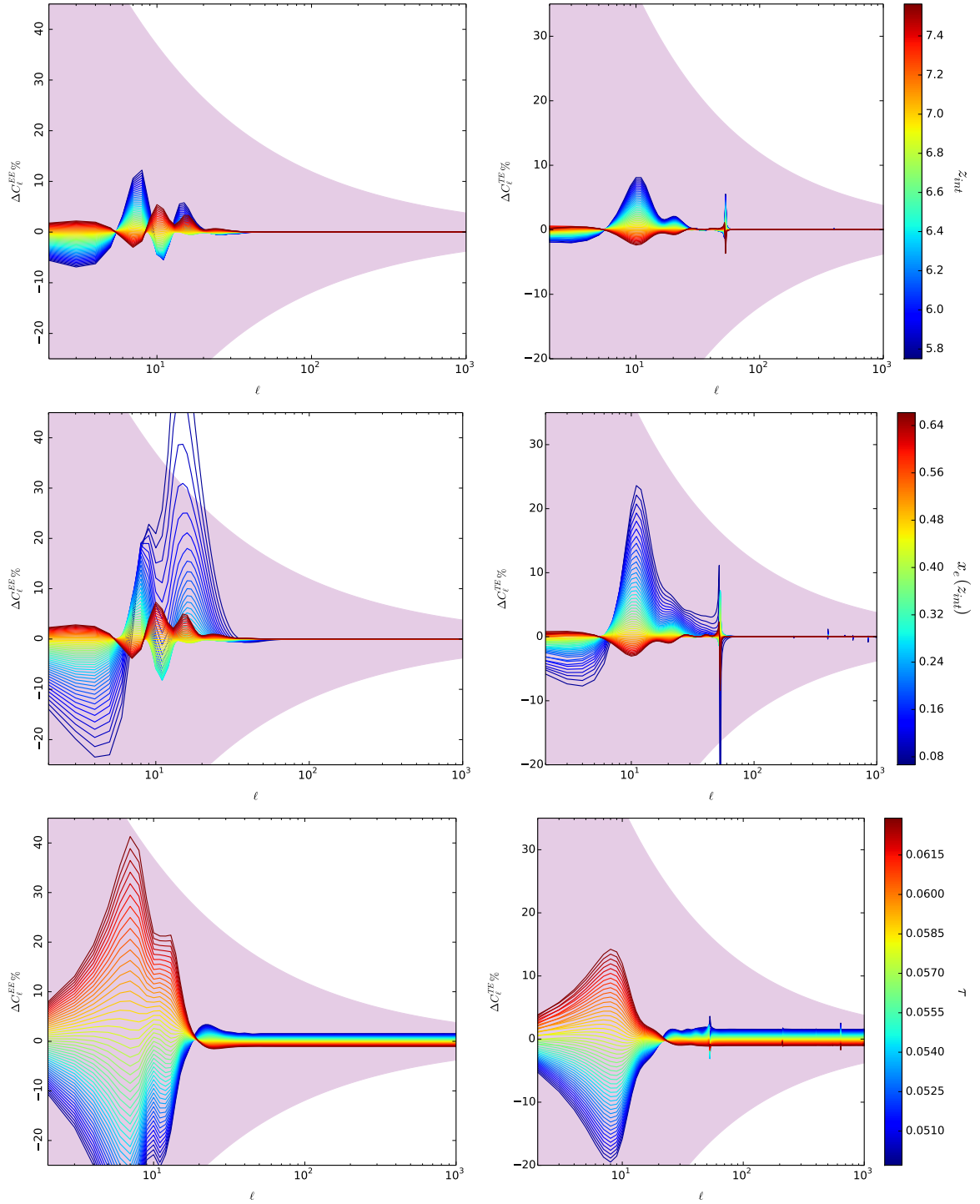


**Figure 2:** Variation of the E-mode polarization and TE cross-correlation angular power spectra with respect to the three Poly-reion parameters. Top panel is the position of the intermediate redshift, second panel is the amplitude the bottom panel is the variation with the optical depth.

of the new Planck 2018 against different models of reionization. Fig. 3 and Fig. 4 summarize the consistency and improvements of the new results.

In Fig. 3 we present the ionization fraction history as constrained from the different data sub-combinations. We note how also for the ionization fraction evolution all the combinations are in good agreement, mirroring the results on the optical depth, with LFI-based results (both 2015 and 2018) allowing for earlier onsets of the reionization with respect to HFI-based data.

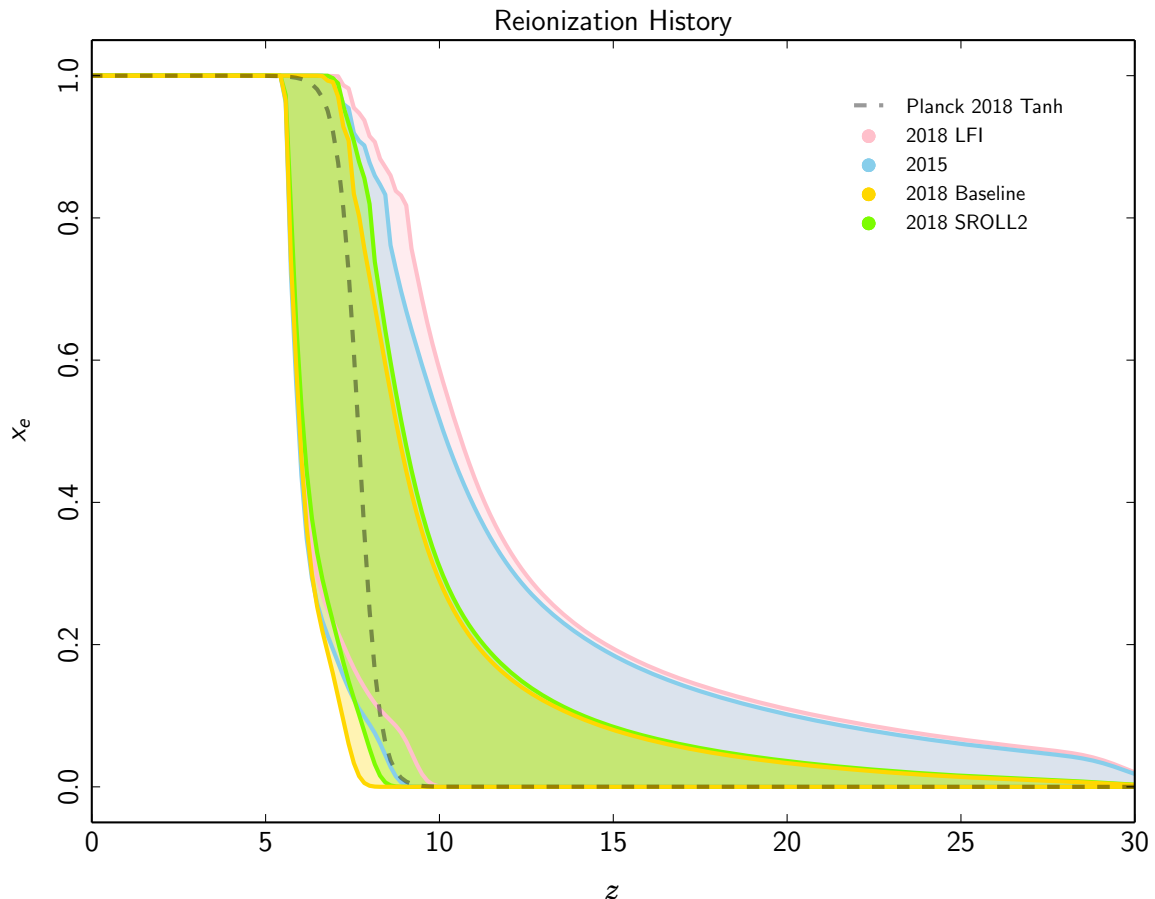


**Figure 3:** Derived 95% confidence limits for  $x_e(z)$  by the Poly-reion model using different Planck 2018 likelihood combinations. The best-fit for  $x_e(z)$  from the Planck 2018 baseline likelihoods in the hyperbolic tangent case is displayed as a dashed line for comparison.

The improvement of Planck 2018 baseline results with respect to the 2015 ones for the hyperbolic tangent is reflected also by a substantial improvement in the constraints on the Poly-reion. In particular, in Fig. 4 we show the comparison of the optical depth as constrained by Planck 2015 and Planck 2018 for the Poly-reion model compared with the analogous for the standard hyperbolic tangent. We note how the tendency to drive upwards the value of the optical depth in the Poly-reion model shown in 2015 data is much reduced with Planck 2018, thanks mainly to the improved polarization data. In the right panel of Fig. 4 we show the comparison of the duration of reionization in Poly-reion between 2015 and 2018. We note that with Planck 2018 the duration of reionization is much tightly constrained ruling out the high redshift tails that were still allowed by Planck 2015 data.

In Fig. 5 we show the breaking of the optical depth versus the scalar spectral index degeneracy, already observed for the hyperbolic tangent, is present also in the Poly-reion model thanks also the tightening in the  $\tau$  direction. We notice also a drastic change in the scatter plot in Fig. 6 with respect to



the analogous of [1] and we especially note again how early onsets are now disfavoured in Poly-reion with Planck 2018 data.

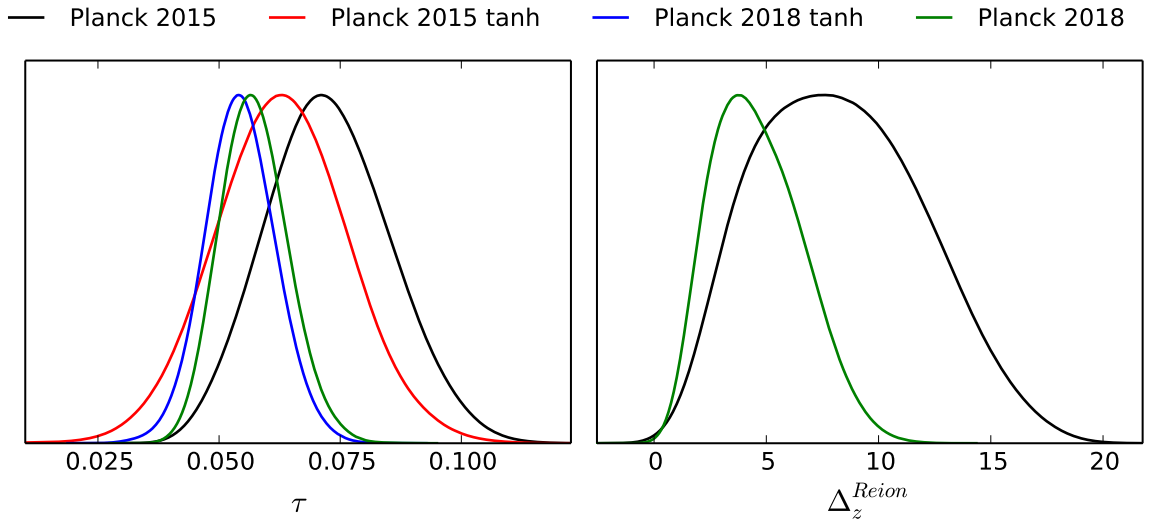


**Figure 4:** Marginalized probability density for  $\tau$  and  $\Delta_z^{Reion}$  for different Planck data. The standard results for  $\tau$  with Planck 2015 (red) and 2018 (blue) are shown for comparison.

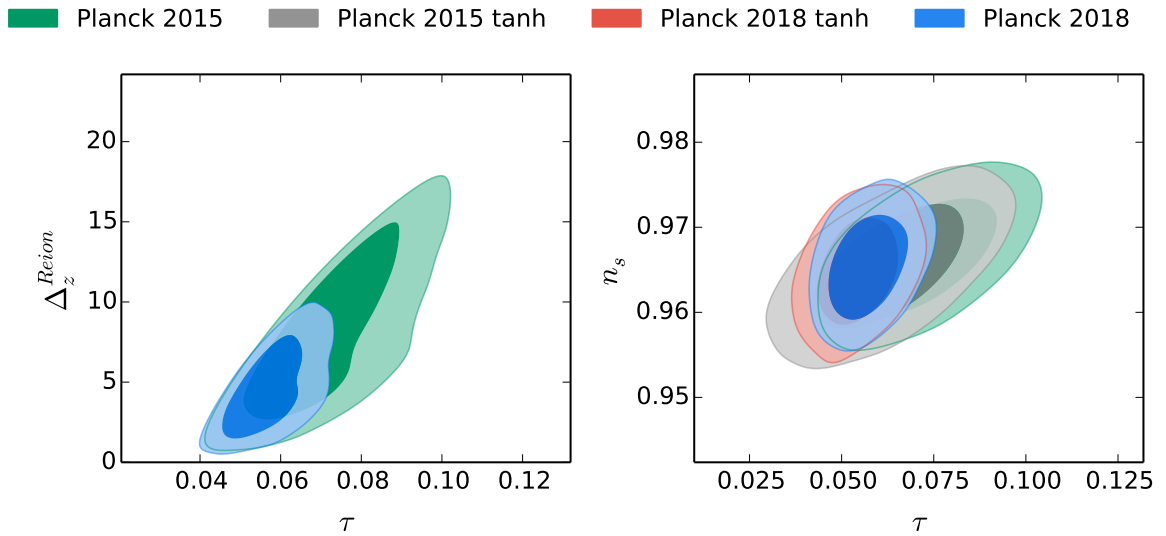


**Figure 5:** Marginalized joint 68% and 95% CL regions for  $(\tau, \Delta_z^{Reion})$  and  $(\tau, n_s)$  with different *Planck* 2018 likelihoods.

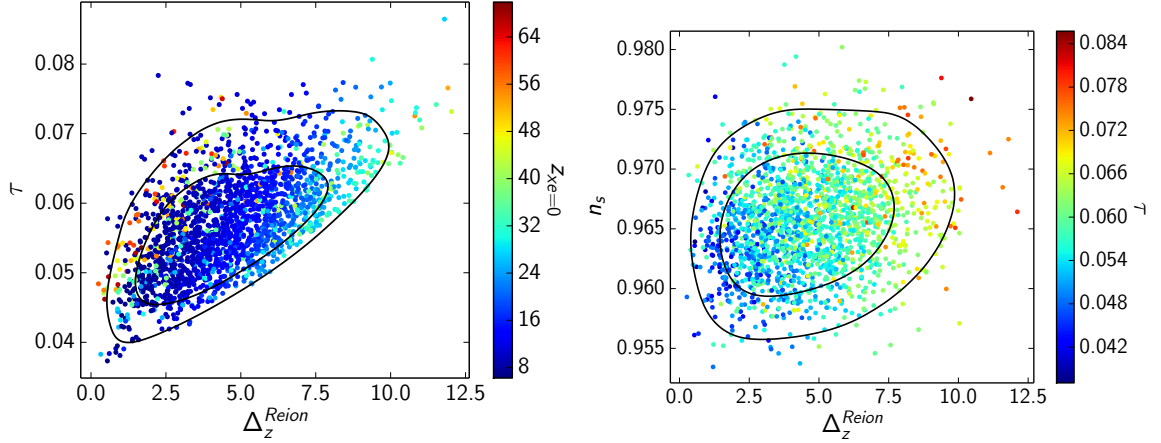


**Figure 6:** Three dimensional posterior distribution for Poly-reion parameters as the duration of reionization and the starting redshift compared with the optical depth and the scalar spectral index for the  $\Lambda$ CDM model.

## 4 Extensions to the $\Lambda$ CDM

We now investigate the constraints of Planck 2018 baseline data on Poly-reion when an extended cosmological model is assumed. We focus on the extended sectors which have known degeneracies with the reionization model updating our previous results with Planck 2015 [1] and adding new cases, such as spatial curvature, number of effective neutrinos and its combination with the sum of neutrino masses, a large scale power suppression and the lensing amplitude.

### 4.1 $\Lambda$ CDM+tensor

We start our compilation of extensions to  $\Lambda$ CDM model by adding a primordial tensor contribution. In this case the main impact is on large angular scales and we expect a slight degeneracy between Poly-reion and the amplitude of tensor modes. We let the tensor to scalar ratio  $r$  free to vary together with the standard cosmological parameters and the Poly-reion ones.

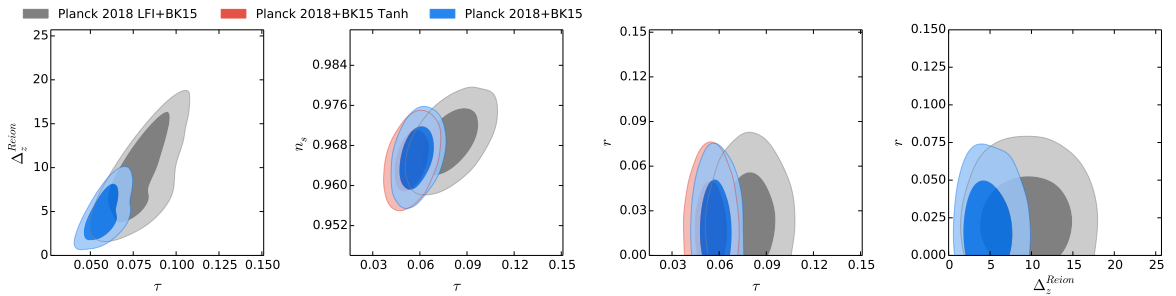


**Figure 7:** Marginalized joint 68% and 95% CL regions for  $(\tau, \Delta_z^{Reion})$ ,  $(\tau, n_s)$ ,  $(\tau, r)$  and  $(r, \Delta_z^{Reion})$  compared with the hyperbolic tangent case.

To add constraining power on the tensor to scalar ratio to the Planck data we combine the Planck 2018 baseline with the Bicep/Keck data on B-mode polarization from 2015 observations[24]. As robustness test we also consider the alternative LFI based Planck 2018 likelihood previously described.

In Table 2 we present the results and in Fig. 7 we show the two dimensional constraints on the reionization parameters and  $r$  compared with the analogous case with the hyperbolic tangent model for reionization. We note that the introduction of the Poly-reion model does not impact the constraints on the tensor to scalar ratio, that are in perfect agreement with the standard case [25]. The two-dimensional posterior distributions do not show any significant degeneracy between the Poly-reion parameters and the tensor to scalar ratio. The use of HFI-based polarization significantly reduces the allowed duration of reionization and delays its onsets with respect to the LFI-based likelihood in the same manner as for the  $\Lambda$ CDM case. We can conclude that the addition of a primordial tensor contribution does not affect either the constraints on primordial tensor amplitudes nor the constraints on the model of reionization.

Parameter/Data	Planck TTTEEE+lowE+lensing+BK15	Planck TTTEEE +LFI+lensing+BK15
$\Omega_b$	$0.0224 \pm 0.0001$	$0.0225 \pm 0.0002$
$\Omega_c$	$0.120 \pm 0.001$	$0.119 \pm 0.001$
$100\theta_{MC}$	$1.0409 \pm 0.0003$	$1.0410 \pm 0.0003$
$\tau$	$0.0581^{+0.0065}_{-0.0077}$	$0.0793^{+0.0119}_{-0.0120}$
$\ln(10^{10}A_s)$	$3.05 \pm 0.01$	$3.09 \pm 0.02$
$n_s$	$0.9657^{+0.0041}_{-0.0042}$	$0.9689 \pm 0.0044$
$r$	$< 0.07$	$< 0.06$
$H_0$	$67.40 \pm 0.54$	$67.97 \pm 0.60$
$z_{re}$	$7.28^{+0.77}_{-1.14}$	$7.95^{+0.83}_{-2.15}$
$z_{xe=0}$	$18.82^{+1.82}_{-11.36}$	$32.13^{+8.71}_{-22.98}$
$\Delta_z^{Reion}$	$4.80^{+1.71}_{-2.47}$	$9.52^{+3.98}_{-4.05}$

**Table 2:** Confidence limits at 68 % (95% for upper limits) for cosmological parameters in the  $\Lambda$ CDM+r model.

## 4.2 Neutrino Physics

We now study how the extension to Poly-reion model for reionization affects the knowledge on neutrino physics from the CMB data.

### 4.2.1 $\Lambda$ CDM+Mnu

We start by assuming a non vanishing neutrino mass. Being Planck data not sensitive to the hierarchy choice, we consider a degenerate hierarchy. We vary the neutrino mass jointly with cosmological and Poly-reion parameters. The resulting two dimensional distributions for the Poly-reion param-

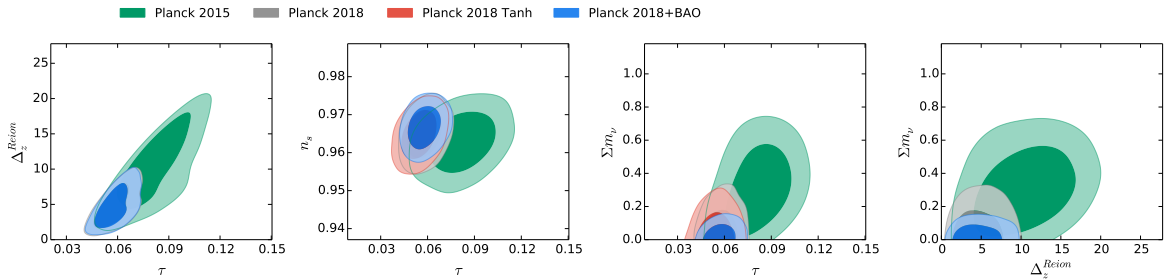


**Figure 8:** Marginalized joint 68% and 95% CL regions for  $(\tau, \Delta_z^{Reion})$ ,  $(\tau, n_s)$ ,  $(\tau, \Sigma m_\nu)$  and  $(\Sigma m_\nu, \Delta_z^{Reion})$  compared with the hyperbolic tangent case and the Planck 2015 results. We also consider the case of the BAO addition in blue.

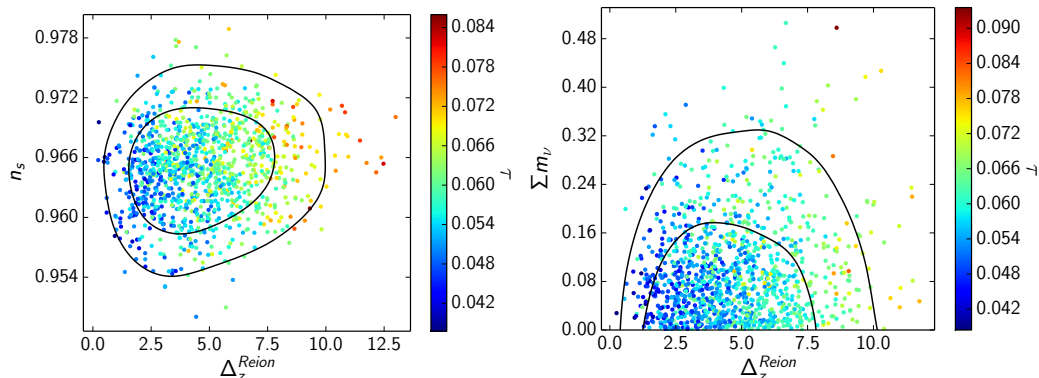


**Figure 9:** Three dimensional marginalized posteriors for the duration of reionization versus the scalar spectral index and the sum of neutrino masses. The color scale is referred to the optical depth.

eters and the neutrino mass are shown in Fig. 8. The resulting constraints on the neutrino mass are  $M_\nu < 0.266$  eV at 95%CL, reduced to  $M_\nu < 0.126$  eV at 95%CL when the Baryonic Acoustic Oscillations data are added to the analysis. The constraints are compatible with the hyperbolic tangent ones, respectively  $M_\nu < 0.24$  eV at 95%CL and  $M_\nu < 0.12$  eV at 95%CL [5]. The minor increase in the upper limit is given by the larger optical depth in Poly-reion, that for the baseline data case is  $\tau = 0.0580^{+0.0067}_{-0.0080}$  at 68%CL with  $z_{xe=0} = 17.92^{+1.47}_{-10.47}$  at 68%CL and  $\Delta_z^{Reion} = 4.71^{+1.60}_{-2.51}$  at 68%CL with only a marginal improvement for the reionization history by the addition of the BAO. The comparison in Fig. 8 between grey, Planck 2018, and green, Planck 2015, contours shows the amazing improvements of Planck 2018 data for this case. In 2015 the strong degeneracy between the neutrino mass and reionization was significantly degrading both constraints on the neutrino sector and reionization. With Planck 2018 data the degeneracy is almost completely broken allowing constraints at the level of the standard hyperbolic tangent. The improvement is also shown in the scatter plot in Fig. 9 where we note the very tight color scale for the optical depth.

#### 4.2.2 $\Lambda$ CDM+ $N_{eff}$

Another degeneracy affecting the neutrino sector and the reionization model is given by the one concerning the additional relativistic degrees of freedom, parametrized by varying the number of effective neutrinos. The grey contours in Fig. 10 shows the constraints of Planck 2015 where the degeneracy is neat. We now test if the degeneracy holds also with Planck 2018 data, the results are

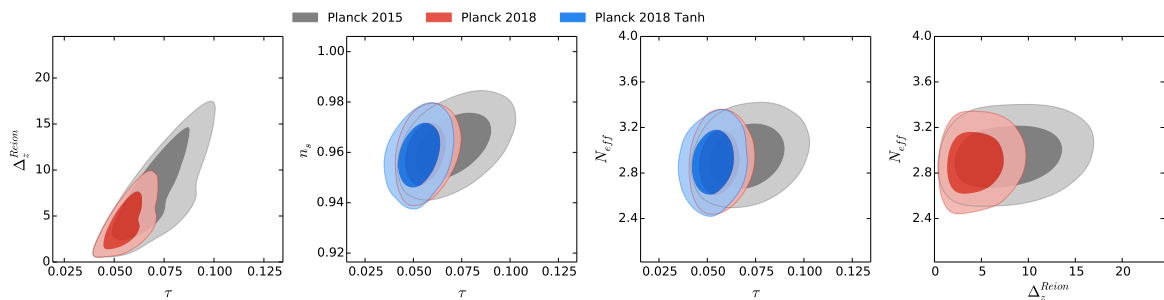


**Figure 10:** Marginalized joint 68% and 95% CL regions for  $(\tau, \Delta_z^{Reion})$ ,  $(\tau, n_s)$ ,  $(\tau, N_{eff})$  and  $(N_{eff}, \Delta_z^{Reion})$  compared with the hyperbolic tangent case and the 2015 results.

presented by the red contours in Fig. 10 were we can already note significant improvement brought

by the new Planck data. The degeneracy is broken and the constraints on the number of effective neutrinos are  $N_{eff} = 2.90 \pm 0.19$  at 68%CL in agreement with  $N_{eff} = 2.89^{+0.19}_{-0.18}$  at 68%CL from the hyperbolic tangent [5]. The optical depth is  $\tau = 0.0564^{+0.0061}_{-0.0076}$  with  $z_{xe=0} = 17.87^{+1.58}_{-10.72}$  and  $\Delta_z^{Reion} = 4.43^{+1.54}_{-2.47}$ .

### 4.2.3 $\Lambda$ CDM+Neff+Mnu

Concluding the overview of the simplest neutrino sector extensions we consider the joint constraints on the number of effective neutrinos and the neutrino mass. In Fig. 11 we show the results for the

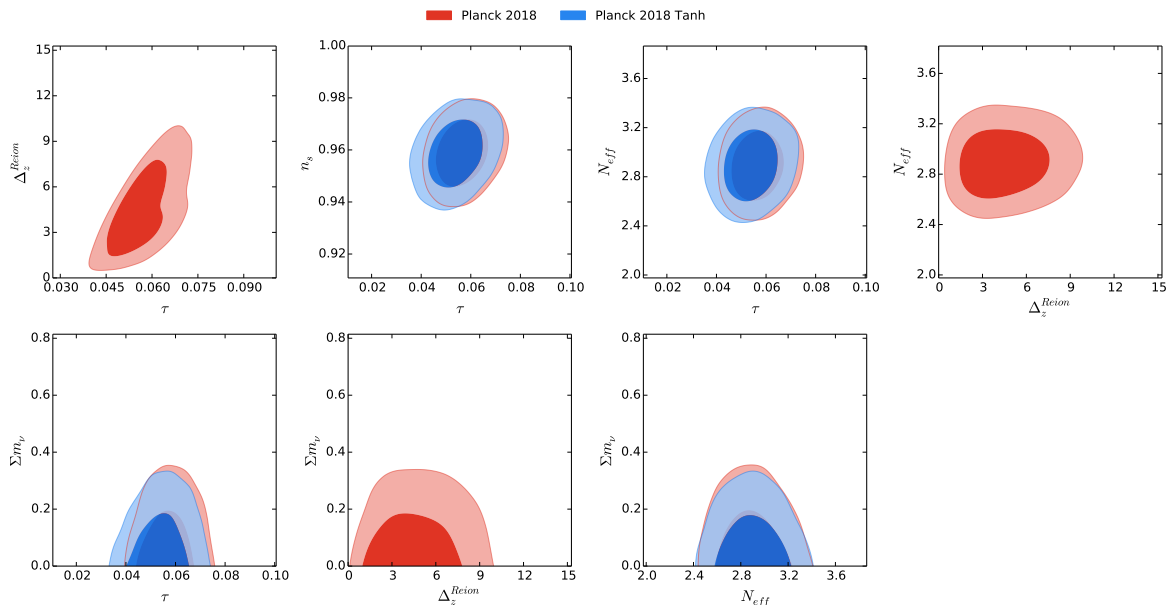


**Figure 11:** Marginalized joint 68% and 95% CL regions for the neutrino sector and Poly-reion parameters compared with the hyperbolic tangent case.

main parameters. We note that also in the case of joint constraints the data are sensitive enough to not suffer from degeneracies and provide constraints on the neutrino physics which are at the same level of the one provided by the standard hyperbolic tangent model:  $N_{eff} = 2.89^{+0.18}_{-0.20}$  at 68% CL and  $M_\nu < 0.28$  to be compared with  $N_{eff} = 2.90^{+0.18}_{-0.19}$  at 68% CL and  $M_\nu < 0.26$  at 95% CL [5]. Concerning the reionization part we note that in comparison with the hyperbolic tangent Poly-reion provides a constraint on  $\tau$  with asymmetric uncertainties  $\tau = 0.0569^{+0.0063}_{-0.0076}$  to be compared with the hyperbolic tangent  $\tau = 0.0539^{+0.0071}_{-0.0072}$  as in previous models [5]. In Table 3 we summarize the results obtained for the physics of neutrinos.

### 4.3 $\Lambda$ CDM+ $A_L$

We proceed by considering the case of the lensing amplitude  $A_L$ . We stress that  $A_L$  is not a physical parameter, it phenomenologically represents the amplitude of the lensing effect on the CMB anisotropy angular power spectra but is not related to the physical lensing signal amplitude, that is measured through the four point correlation function on maps and that is at the base of the lensing likelihood [21]. In order to study the correlation between the reionization history and the  $A_{lens}$  without biases we do not include the lensing likelihood in the following analysis.

The reason beyond considering this specific extension of the  $\Lambda$ CDM is that although  $A_L$  is not physical parameter it's a tracer of possible effects in the high multipoles region of the CMB angular

Parameter/Model	$\Lambda$ CDM+ $\Sigma m_\nu$	$\Lambda$ CDM+ $N_{eff}$	$\Lambda$ CDM+ $\Sigma m_\nu$ + $N_{eff}$
$\tau$	$0.0580^{+0.0067}_{-0.0080}$	$0.0564^{+0.0061}_{-0.0076}$	$0.0569^{+0.0063}_{-0.0076}$
$M_\nu$	$< 0.266$	-	$< 0.28$
$N_{eff}$	-	$2.90 \pm 0.19$	$2.89^{+0.18}_{-0.20}$
$\ln(10^{10})$	$3.052^{+0.014}_{-0.016}$	$3.042^{+0.015}_{-0.017}$	$3.043^{+0.015}_{-0.018}$
$n_s$	$0.9650 \pm 0.0042$	$0.9596 \pm 0.0081$	$0.9590 \pm 0.0085$
$z_{re}$	$7.34^{+0.80}_{-1.07}$	$7.15^{+0.67}_{-1.08}$	$7.19^{+0.69}_{-1.13}$
$z_{xe=0}$	$17.92^{+1.47}_{-10.47}$	$17.87^{+1.58}_{-10.72}$	$18.27^{+1.67}_{-11.00}$
$\Delta_z^{Reion}$	$4.71^{+1.60}_{-2.51}$	$4.43^{+1.54}_{-2.47}$	$4.54^{+1.61}_{-2.49}$

**Table 3:** Confidence limits at 68% ( 95% for upper bounds) for neutrino sector parameters within the Poly-reion model.

power spectra and in particular of smoothing/oscillatory patterns in the acoustic peaks region. For this reason it can be degenerate with the effect of reionization on high multipoles, in particular when it's considered an extended cosmological model. We also remind that its value in the Planck 2018 baseline with the hyperbolic tangent is slightly higher than unity  $A_L = 1.180 \pm 0.065$  at 65% CL indicating a preference of Planck data for an higher lensing smoothing than predicted [5]. When

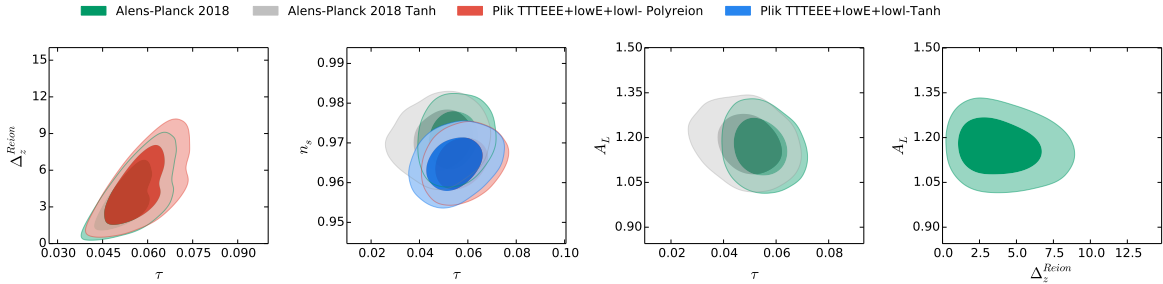


**Figure 12:** Marginalized joint 68% and 95% CL regions for  $(\tau, \Delta_z^{Reion})$ ,  $(\tau, n_s)$ ,  $(\tau, A_L)$  and  $(A_L, \Delta_z^{Reion})$  compared with the hyperbolic tangent case and the LCDM.

adding the  $A_L$  parameter to the Poly-reion framework we obtain a slightly lower value with respect to the hyperbolic tangent, namely  $A_L = 1.17^{+0.06}_{-0.07}$  at 68% CL, with similar uncertainty. In Fig. 12 we can see the drag of the Poly-reion model on the  $A_L$  parameter by comparing the green contour with the analogous in hyperbolic tangent in red. The Poly-reion preference for higher optical depths together with the freedom in the duration of reionization, not allowed in the hyperbolic tangent (where the  $\Delta_z^{Reion}$  is fixed), decreases the widening of the optical depth posterior and its pull towards lower values given by the inclusion of the lensing amplitude. In fact, with Poly-reion we have  $\tau = 0.054^{+0.006}_{-0.008}$  at 68% CL whereas the hyperbolic tangent provides  $\tau = 0.049^{+0.009}_{-0.007}$  at 68% CL. The uncertainties are almost comparable but the asymmetry in the error bars have opposite directions. In Fig. 12 we compare the  $\Lambda$ CDM+ $A_L$  case with the standard  $\Lambda$ CDM results, we note that also for the Poly-reion model we have a pull of  $A_L$  towards lower values of the optical depth as in the hyperbolic tangent, but the structure of Poly-reion somehow limits this pull.

#### 4.4 $\Lambda$ CDM+curvature

Another model which is sensitive to possible effects in the region of the acoustic peaks is the non-flat geometry. Also in this case the Planck results have consistently preferred negative values of the curvature parameter, being  $\Omega_k = -0.044^{+0.018}_{-0.015}$  [5] the Planck 2018 results, corresponding to preference for a closed universe model. The addition of the lensing brings the value in full agreement

with a flat universe but since we want to investigate the correlation of the spatial curvature with the Poly-reion model of reionization also in this case we exclude the lensing likelihood from the analysis. As expected the results show an analogous behaviour to the ones with the addition of  $A_L$  as presented

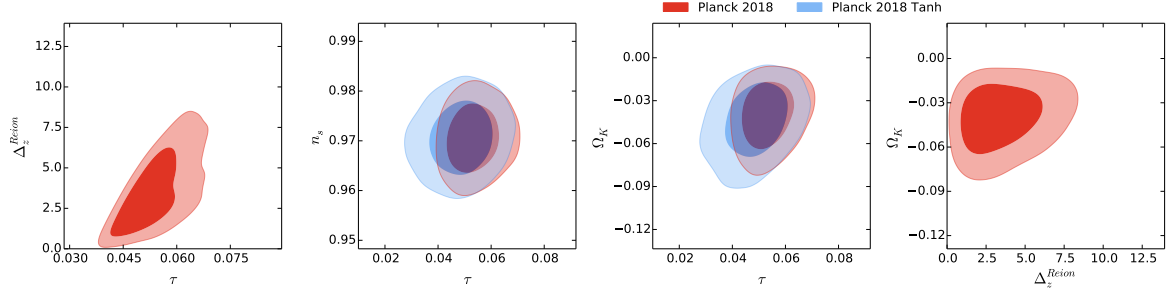


**Figure 13:** Marginalized joint 68% and 95% CL regions for  $(\tau, \Delta_z^{Reion})$ ,  $(\tau, n_s)$ ,  $(\tau, \Omega_k)$  and  $(\Omega_k, \Delta_z^{Reion})$  compared with the hyperbolic tangent case.

in Fig. 13. We note how also for this case the pull towards lower values of the optical depth given by the addition of the curvature in the Poly-reion model  $\tau = 0.053^{+0.006}_{-0.007}$  is reduced with respect to the hyperbolic tangent case  $\tau = 0.049^{+0.007}_{-0.008}$  with slightly smaller error bars for the Poly-reion case. The reduced pull towards lower values is reflected in a slightly higher value of the spatial curvature  $\Omega_K = -0.040^{+0.017}_{-0.014}$  at 68% CL and slightly smaller error bars.

#### 4.5 Large scale power suppression

We now consider a possible variation to the initial power spectrum of primordial perturbations that wants to phenomenologically represent the power suppression observed on large angular scales in the CMB angular power spectra. We model this effect by inserting a cut off into the primordial power spectrum for cosmological perturbations that takes the form [25]:

$$P(k) = P_0(k) \left[ 1 - \exp\left(-\left(\frac{k}{k_c}\right)^{\lambda_c}\right) \right], \quad (4.1)$$

where  $P_0(k)$  is the standard power law primordial power spectrum. In order to reduce the parameter space, we consider the specific case of  $\lambda_c = 3.35$ . The results are presented in Fig. 14. We do not note any significant degeneracy among the Poly-reion parameters and the cut off pivot scale. The

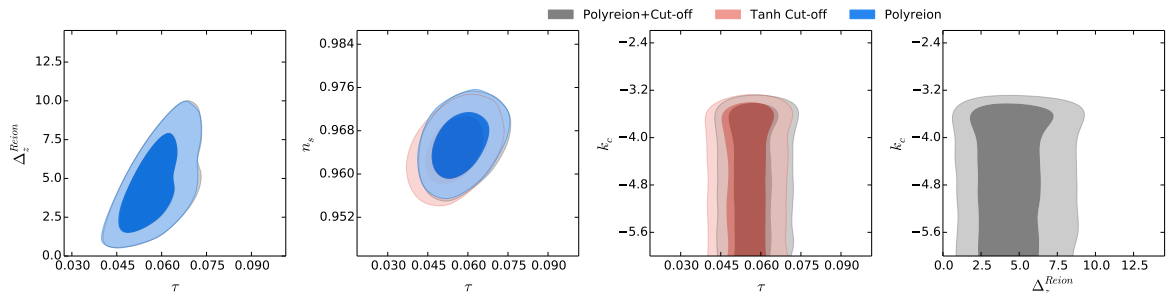


**Figure 14:** Marginalized joint 68% and 95% CL regions for  $(\tau, \Delta_z^{Reion})$ ,  $(\tau, n_s)$ ,  $(\tau, k_c)$  and  $(k_c, \Delta_z^{Reion})$  in large scale power suppression model for the primordial power spectrum. The results for this model are compared with the standard Poly-reion case.

constraints on the Poly-reion parameters are the same as in the standard primordial power spectrum

case showing again also for this extension that there are no strong degeneracies with Planck 2018 data.

#### 4.6 $\Lambda$ CDM+DM annihilation

We conclude our review of some of the main correlations of extended cosmological models with the Poly-reion by considering the contribution of dark matter annihilation to the cosmological environment [5, 26–31, 34]. Annihilating DM has a twofold effect on CMB anisotropies. On one side, the annihilated DM particles do not participate anymore to the matter budget of the Universe, decreasing the DM overall contribution to CMB and in particular to the acoustic peaks structure. On the other side, the annihilated DM has not disappeared but has been converted into additional radiation that is injected into the cosmological plasma. As for other forms of additional radiation or energy injections (e.g. the dissipation of primordial magnetic fields [32]) this process modifies the ionization fraction evolution. This direct effect on the ionization fraction is the main reason why DM annihilation is degenerate with extended histories of reionization which phenomenologically reconstruct the ionization fraction evolution [1].

The main free parameter describing the DM annihilation is the cross section usually parametrized as:

$$p_{ann} = \frac{f_{eff}\langle\sigma v\rangle}{m_\chi} \quad (4.2)$$

where we have the particle mass at denominator and the thermally averaged annihilation cross-section;  $f_{eff}$  is the fraction of the energy released and transferred to the plasma at redshift 600. We use the Cosmorec [33] extension which includes the injection of energy by dark matter annihilation in the plasma [34] that varies the parameter  $\epsilon_0 f_d$  that is related to the  $p_{ann}$  by  $p_{ann}[\times 10^{-28} \text{cm}^3/\text{s}/\text{GeV}] \sim 10\epsilon_0 f_d (0.13/\omega_c h^2)^2$ . In Fig. 15 we present the results, Planck 2018 data constrain  $\epsilon_0 f_d < 0.3$  that

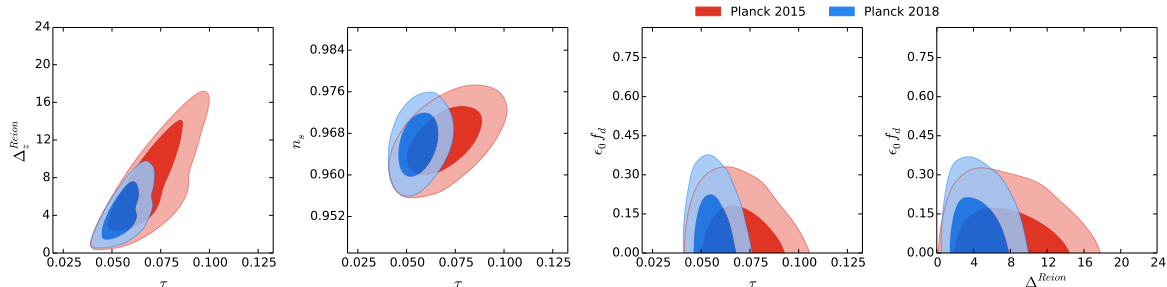


**Figure 15:** TMarginalized joint 68% and 95% CL regions for  $(\tau, \Delta_z^{Reion})$ ,  $(\tau, n_s)$ ,  $(\tau, \epsilon_0 f_d)$  and  $(\epsilon_0 f_d, \Delta_z^{Reion})$  compared with the hyperbolic tangent case.

corresponds to  $p_{ann}[\times 10^{-28} \text{cm}^3/\text{s}/\text{GeV}] < 4$  at 95% CL. The Poly-reion case is in agreement with, although slightly worse than, the hyperbolic tangent case which gives  $p_{ann}[\times 10^{-28} \text{cm}^3/\text{s}/\text{GeV}] < 3.3$  at 95% CL [5]. If we compare the Poly-reion results with Planck 2018 and Planck 2015 shown in red in figure, we note that among all the Poly-reion extended cosmological models we have considered, the DM annihilation is the only one where we have a degradation of the constraint with respect to 2015 that gave  $p_{ann}[\times 10^{-28} \text{cm}^3/\text{s}/\text{GeV}] < 3$  at 95% CL [1]. Although the DM annihilation constraint is slightly degraded, the Planck 2018 determination of the optical depth, i.e.  $\tau = 0.056 \pm 0.007$  at 68% CL, improves on the corresponding 2015 value in the DM annihilation model, i.e.  $\tau = 0.070^{+0.012}_{-0.013}$ . The degradation of the constraint on the DM annihilation cross section may be indeed driven by a combination of the lowering of the value of the optical depth and its halved error bars that may have caused the correlation of the two parameters to move towards higher cross sections for DM.



In summary, the use of Planck 2018 baseline likelihoods remove most of the remaining degeneracies between the physics of reionization and the extended cosmological models we consider. In particular, the reionization parameters seem to decouple from the neutrino sector, the primordial tensor modes and a suppression of power at the largest scales and a small degeneracy seems to remain for the spatial curvature, a variable lensing amplitude and the contribution of annihilating dark matter. It is conceivable that the baseline Planck 2018 likelihood lowE, empirically obtained by simulations within  $\Lambda$ CDM, could contribute to the stability of the constraints on reionization parameters in extended cosmological models compared to  $\Lambda$ CDM.

## 5 Conclusions

Thanks to the update of the large scale polarization from HFI and in particular the likelihood based on the 100x143 GHz cross angular power spectrum, Planck 2018 data made possible to investigate the history of reionization in great details. In the framework of the standard hyperbolic tangent model for the reionization history Planck 2018 data have led to a lower value of  $\tau$  with a significant reduction in its uncertainty, i.e.  $0.053 \pm 0.009$  with only lowE and  $0.0544 \pm 0.0073$  with the "baseline" combination including temperature, polarization and lensing [5]. In [5] are also presented the constraints on extended reionization by PCA [35, 36] and Flexknot [8] approaches from the large angular scale E-mode polarization with the other cosmological parameters fixed.

We have studied the constraints with Planck 2018 data on the reionization history when it is modelled with Poly-reion [2] with flexible node [1]. This model by construction allows more freedom both in the duration of reionization and its phenomenology than the standard hyperbolic tangent model. The results on the  $\Lambda$ CDM model obtained by different combinations of Planck 2018 subsets of data show a great improvement with respect to the Planck 2015 results [1]. The Poly-reion estimate of the optical depth is in agreement with the hyperbolic tangent model with a similar uncertainty, i.e.  $\tau = 0.0572^{+0.0064}_{-0.0075}$  at 68 % CL. By using Poly-reion we find a significant reduction of the allowed duration of reionization compared to Planck 2015 data, i.e.  $\Delta_z^{Reion} = 4.6^{+1.7}_{-2.5}$  at 68% CL, and that very early onsets are now disfavoured by Planck 2018 data.

We find consistent results within the Planck 2018 baseline likelihoods and between Planck 2018 baseline and alternative likelihoods, such as the LFI low-resolution joint ( $T, Q, U$ ) likelihood. We have also analyzed the update of the HFI data processing from the SROLL2 map making algorithm [16]: we find  $\tau = 0.0600^{+0.0052}_{-0.0064}$ , still consistent with the corresponding hyperbolic tangent result  $\tau = 0.0590^{+0.0058}_{-0.0068}$  [23] (with a very small improvement due to the addition of the lensing likelihood in the Poly-reion results).

Models of the reionization history which allow for more freedom than the standard hyperbolic tangent may worsen the degeneracies between the reionization and cosmological model beyond  $\Lambda$ CDM. We have considered some of the main extensions to the  $\Lambda$ CDM that are known to be degenerate with the physics of reionization. We updated our previous results with Planck 2015 [1] and we have also considered models with both neutrino number and mass allowed to vary, the addition of the CMB lensing amplitude  $A_L$ , a primordial tensor contribution and finally the spatial curvature. The results show that all the degeneracies are broken for both the neutrino physics sector and the primordial tensor contributions, providing constraints in perfect agreement with the one given by the hyperbolic tangent model. Some residual degeneracy is present instead for the lensing amplitude and the spatial curvature. In these models the use of the Poly-reion, for its tendency to increase the value of the optical depth, decreases the pull of the extended model towards lower values of the optical depth causing the degeneracy to shift the values of both the lensing amplitude and the spatial curvature towards  $\Lambda$ CDM case. The DM annihilation is the only model where we have degradation of the

constraint with Planck 2018 with respect to Planck 2015 for the additional parameter of the model, we note however the improvement on the optical depth determination within this model.

In Figure 16 we summarize the constraints on the Poly-reion reionization history in the framework of the cosmological models we have considered by showing the evolution of the ionization fractions. The comparison with the Poly-reion  $\Lambda$ CDM case reflects the results on the cosmological parameters with the neutrino physics being in perfect agreement whereas the spatial curvature and lensing amplitude prefers slightly more recent onsets of the reionization in agreement with a lower value of the optical preferred by these models.

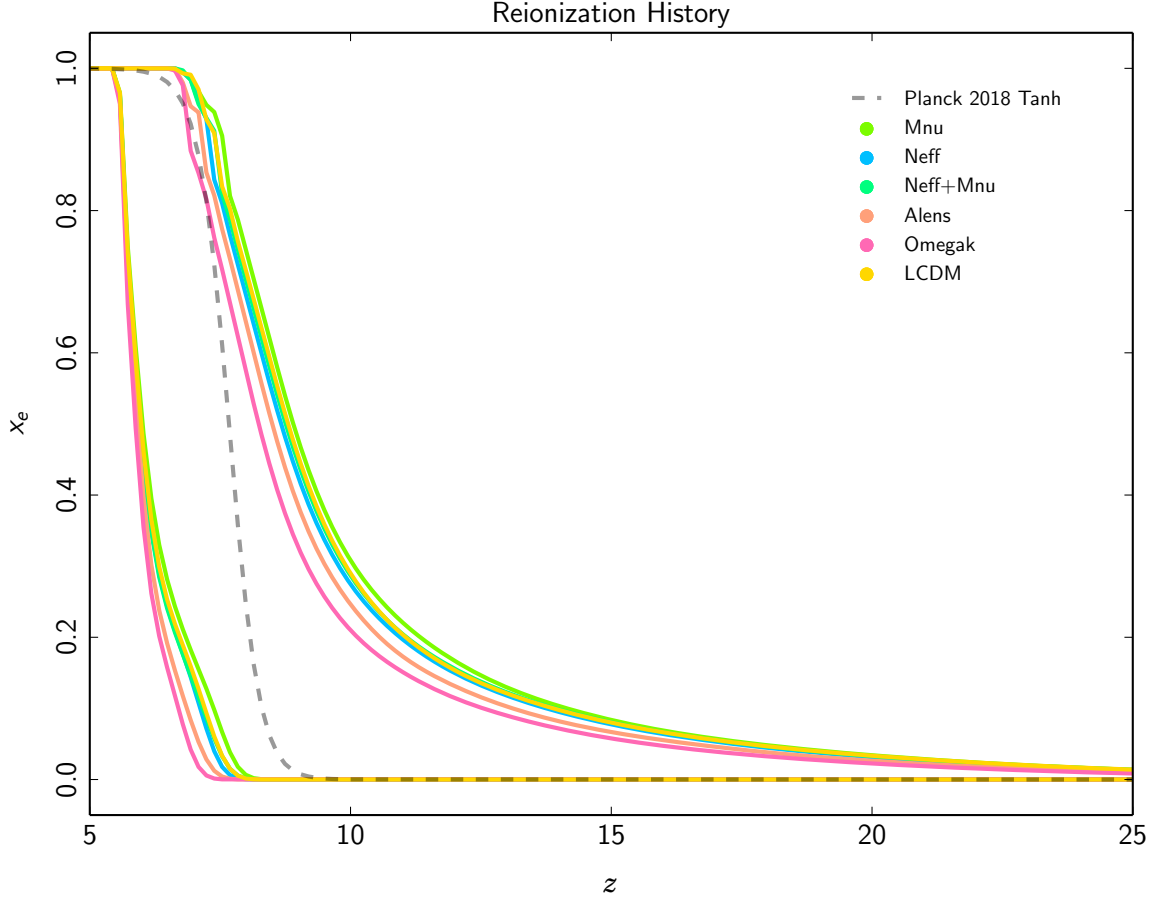


**Figure 16:** 95% CL bands for the ionization fraction as a function of redshift as reconstructed for a subset of the extensions to the  $\Lambda$ CDM considered in this work in different colours.

The understanding of the history of reionization is one of the main scientific targets of future CMB experiments from space thanks to the cosmic variance limited measurement of the E-mode polarization on a wide range of multipoles, including the reionization bump at the lowest multipoles. Future experiments like the LiteBIRD satellite [37] will provide a cosmic variance limited measurement of the optical depth,  $\sigma(\tau) \sim 0.002$  and provide tight constraints on the duration of reionization see [1] for some detailed forecasts.

## Acknowledgments

We would like to thank Luca Pagano for the useful discussions and for helping in the use of SROLL2 likelihood. DP and FF acknowledge financial support by ASI Grant 2016-24-H.0. This research used computational resources provided by INAF OAS Bologna and by CINECA under the agreement with INFN. DKH has received fundings from the European Unions Horizon 2020 research and innovation programme under the Marie Skłodowska-Curie grant agreement No. 664931.

## References

- [1] D. K. Hazra, D. Paoletti, F. Finelli and G. F. Smoot, *JCAP* **1809** (2018) 016 doi:10.1088/1475-7516/2018/09/016 [arXiv:1807.05435 [astro-ph.CO]].
- [2] D. K. Hazra and G. F. Smoot, *JCAP* **1711** (2017) 028 doi:10.1088/1475-7516/2017/11/028 [arXiv:1708.04913 [astro-ph.CO]].
- [3] Planck Collaboration, *Astron. Astrophys.* **596** (2016) A107 doi:10.1051/0004-6361/201628890 [arXiv:1605.02985 [astro-ph.CO]].
- [4] Planck Collaboration *Astron. Astrophys.* **596** (2016) A108 doi:10.1051/0004-6361/201628897 [arXiv:1605.03507 [astro-ph.CO]].
- [5] Planck Collaboration, arXiv:1807.06209 [astro-ph.CO].
- [6] C. H. Heinrich, V. Miranda and W. Hu, *Phys. Rev. D* **95** (2017) no.2, 023513 doi:10.1103/PhysRevD.95.023513 [arXiv:1609.04788 [astro-ph.CO]].
- [7] C. Heinrich and W. Hu, *Phys. Rev. D* **98** (2018) no.6, 063514 doi:10.1103/PhysRevD.98.063514 [arXiv:1802.00791 [astro-ph.CO]].
- [8] M. Millea and F. Bouchet, *Astron. Astrophys.* **617** (2018) A96 doi:10.1051/0004-6361/201833288 [arXiv:1804.08476 [astro-ph.CO]].
- [9] A. Gorce, M. Douspis, N. Aghanim and M. Langer, *Astron. Astrophys.* **616** (2018) A113 [*Astron. Astrophys.* **616** (2018) A113] doi:10.1051/0004-6361/201629661 [arXiv:1710.04152 [astro-ph.CO]].
- [10] D. K. Hazra, D. Paoletti, F. Finelli and G. F. Smoot, arXiv:1904.01547 [astro-ph.CO].
- [11] S. Mitra, T. R. Choudhury and A. Ferrara, *Mon. Not. Roy. Astron. Soc.* **454** (2015) no.1, L76 doi:10.1093/mnras/1slv134 [arXiv:1505.05507 [astro-ph.CO]].
- [12] G. Efstathiou and J. Bond, *Mon. Not. Roy. Astron. Soc.* **304** (1999), 75-97 doi:10.1046/j.1365-8711.1999.02274.x [arXiv:astro-ph/9807103 [astro-ph]].
- [13] C. Howlett, A. Lewis, A. Hall and A. Challinor, *JCAP* **04** (2012), 027 doi:10.1088/1475-7516/2012/04/027 [arXiv:1201.3654 [astro-ph.CO]].
- [14] D. K. Hazra, D. Paoletti, M. Ballardini, F. Finelli, A. Shafieloo, G. F. Smoot and A. A. Starobinsky, *JCAP* **1802** (2018) 017 doi:10.1088/1475-7516/2018/02/017 [arXiv:1710.01205 [astro-ph.CO]].
- [15] M. J. Mortonson, C. Dvorkin, H. V. Peiris and W. Hu, *Phys. Rev. D* **79** (2009) 103519 doi:10.1103/PhysRevD.79.103519 [arXiv:0903.4920 [astro-ph.CO]].
- [16] J.-M. Delouis, L. Pagano, S. Mottet, J.-L. Puget and L. Vibert, *Astron. Astrophys.* **629** (2019) A38 doi:10.1051/0004-6361/201834882 [arXiv:1901.11386 [astro-ph.CO]].
- [17] F. N. Fritsch and R. E. Carlson, *SIAM J. Numerical Analysis*, **17**, (1980), pp.238-246. [18]
- [18] J. Schroeder, A. Mesinger and Z. Haiman, *Mon. Not. Roy. Astron. Soc.* **428** (2013), 3058 doi:10.1093/mnras/sts253 [arXiv:1204.2838 [astro-ph.CO]].
- [19] I. McGreer, A. Mesinger and V. D’Odorico, *Mon. Not. Roy. Astron. Soc.* **447** (2015) no.1, 499-505 doi:10.1093/mnras/stu2449 [arXiv:1411.5375 [astro-ph.CO]].

- [20] Planck Collaboration, arXiv:1907.12875 [astro-ph.CO].
- [21] Planck Collaboration, arXiv:1807.06210 [astro-ph.CO].
- [22] U. Natale, L. Pagano, M. Lattanzi, M. Migliaccio, L. Colombo, A. Gruppuso, P. Natoli and G. Polenta, [arXiv:2005.05600 [astro-ph.CO]].
- [23] L. Pagano, J.-M. Delouis, S. Mottet, J.-L. Puget and L. Vibert, arXiv:1908.09856 [astro-ph.CO].
- [24] P. A. R. Ade *et al.* [BICEP and Keck Collaborations], arXiv:1807.02199 [astro-ph.CO].
- [25] Planck Collaboration, arXiv:1807.06211 [astro-ph.CO].
- [26] S. Galli, F. Iocco, G. Bertone and A. Melchiorri, Phys. Rev. D **80** (2009) 023505 doi:10.1103/PhysRevD.80.023505 [arXiv:0905.0003 [astro-ph.CO]].
- [27] S. Galli, T. R. Slatyer, M. Valdes and F. Iocco, Phys. Rev. D **88** (2013) 063502 doi:10.1103/PhysRevD.88.063502 [arXiv:1306.0563 [astro-ph.CO]].
- [28] L. Lopez-Honorez, O. Mena, S. Palomares-Ruiz and A. C. Vincent, JCAP **1307**, 046 (2013) doi:10.1088/1475-7516/2013/07/046 [arXiv:1303.5094 [astro-ph.CO]].
- [29] M. Kawasaki, K. Nakayama and T. Sekiguchi, Phys. Lett. B **756**, 212 (2016) doi:10.1016/j.physletb.2016.03.005 [arXiv:1512.08015 [astro-ph.CO]].
- [30] Planck Collaboration XIII, Astron. Astrophys. **594**, A13 (2016) doi:10.1051/0004-6361/201525830 [arXiv:1502.01589 [astro-ph.CO]].
- [31] E. Di Valentino *et al.* [CORE Collaboration], JCAP **1804**, 017 (2018) doi:10.1088/1475-7516/2018/04/017 [arXiv:1612.00021 [astro-ph.CO]].
- [32] D. Paoletti, J. Chluba, F. Finelli and J. A. Rubino-Martin, Mon. Not. Roy. Astron. Soc. **484** (2019) no.1, 185 doi:10.1093/mnras/sty3521 [arXiv:1806.06830 [astro-ph.CO]].
- [33] J. Chluba and R. M. Thomas, Mon. Not. Roy. Astron. Soc. **412**, 748 (2011) doi:10.1111/j.1365-2966.2010.17940.x [arXiv:1010.3631 [astro-ph.CO]]; Y. Ali-Haïmoud and C. M. Hirata, Phys. Rev. D **82**, 063521 (2010) doi:10.1103/PhysRevD.82.063521 [arXiv:1006.1355 [astro-ph.CO]]; J. Chluba, G. M. Vasil and L. J. Dursi, Mon. Not. Roy. Astron. Soc. **407**, 599 (2010) doi:10.1111/j.1365-2966.2010.16940.x [arXiv:1003.4928 [astro-ph.CO]]; E. R. Switzer and C. M. Hirata, Phys. Rev. D **77**, 083006 (2008) doi:10.1103/PhysRevD.77.083006 [astro-ph/0702143 [ASTRO-PH]]; D. Grin and C. M. Hirata, Phys. Rev. D **81**, 083005 (2010) doi:10.1103/PhysRevD.81.083005 [arXiv:0911.1359 [astro-ph.CO]]; J. A. Rubino-Martin, J. Chluba, W. A. Fendt and B. D. Wandelt, Mon. Not. Roy. Astron. Soc. **403**, 439 (2010) doi:10.1111/j.1365-2966.2009.16136.x [arXiv:0910.4383 [astro-ph.CO]].
- [34] J. Chluba, Mon. Not. Roy. Astron. Soc. **402** (2010) 1195 doi:10.1111/j.1365-2966.2009.15957.x [arXiv:0910.3663 [astro-ph.CO]].
- [35] W. Hu and G. P. Holder, Phys. Rev. D **68** (2003) 023001 doi:10.1103/PhysRevD.68.023001
- [36] M. J. Mortonson and W. Hu, Astrophys. J. **672** (2008) 737 doi:10.1086/523958
- [37] M. Hazumi *et al.*, J. Low. Temp. Phys. **194** (2019) no.5-6, 443. doi:10.1007/s10909-019-02150-5